Catalase Modeling. 2. Dynamics of Reaction of a Water-Soluble and Non μ-Oxo Dimer Forming Manganese(III) Porphyrin with Hydrogen Peroxide

P. N. Balasubramanian, Ernst S. Schmidt, and Thomas C. Bruice*

Contribution from the Department of Chemistry, University of California at Santa Barbara, Santa Barbara, California 93106. *Received April 16, 1987*

Abstract: The catalase-like conversion of hydrogen peroxide to water and oxygen has been studied between pH 7.6 and 12.1 (μ = 0.23) using as catalyst the water-soluble and non μ-oxo dimer forming aquo[5,10,15,20-tetrakis(2,6-dimethyl-3-sulfonatophenyl)porphinato]manganese(III) [i.e., (**1**)Mn^{III}(X), X = H_2O, HO^-]. 2,2′-Azinobis(3-ethylbenzthiazolinesulfonic acid) (ABTS), which undergoes 1e oxidation to the stable radical $ABTS^{\bullet+}$, was used as a partial trap of the intermediate higher valent manganese–oxo porphyrin. Under the conditions $[H_2O_2] > [(1)Mn^{III}(X)] < [ABTS]$, the formation of the products O_2 and $ABTS^{\bullet+}$ follows the first-order rate law. The pseudo-first-order rate constants (k_{obsd}) are linearly dependent upon $[(1)Mn^{III}(X)]$ ($k_{obsd}/[(1)Mn^{III}(X)] = k_{1y}$ M^{-1} s^{-1}) but independent of $[H_2O_2]_T$ and [ABTS]. Thus, the rate-limiting step is oxygen transfer from hydrogen peroxide to manganese(III) porphyrin to provide a 2e-oxidized manganese–oxo species, which then rapidly oxidizes ABTS to $ABTS^{\bullet+}$ and hydrogen peroxide to O_2 and water. The compositions of critical complexes and the product of the equilibrium constants for their formation and rate constants for their decay were determined from the log k_{1y} vs pH profile as follows: Ia, $(1)Mn^{III}(OH)(H_2O_2)$, 87.6 M^{-1} s^{-1} (or Ib, $(1)Mn^{III}(H_2O)(HO_2)$); II, $(1)Mn^{III}(HO)(HO_2)$, 5.38 × 10^4 M^{-1} s^{-1}; III, $(1)Mn^{III}(HO)_2(HO_2)$, 6.94 × 10^5 M^{-1} s^{-1}. The product formed by oxygen transfer from the hydrogen peroxide moiety on decomposition of Ia (and Ib) is likely a manganese(IV)–oxo porphyrin π-cation radical $[(^{+\bullet}1)Mn^{IV}O(Y)$ (Y = HO^- or $(HO^-)_2$)], while decompositions of II and III are presumed to yield manganese(V)–oxo porphyrins $[(1)Mn^{V}(O)(HO)$ and $(1)Mn^{V}(O)(OH)_2$, respectively]. The oxygen-transfer reactions are not subject to general-base catalysis by $H_2PO_4^-$, HPO_4^{2-}, HCO_3^-, CO_3^{2-}, imidazole (ImH), or 2,4,6-collidine. Comparison of the rate constants for oxygen transfer from HO_2^- to $(1)Mn^{III}(HO)$ and to $(1)Mn^{III}(ImH)$ (5.6×10^5 M^{-1} s^{-1}) shows that the reaction with the ImH-ligated species is but ~10-fold greater. Comparison of the pH dependence of the relative rates of ABTS 1e oxidation to $ABTS^{\bullet+}$ and O_2 formation by 2e oxidation of hydrogen peroxide establishes that ABTS oxidation is favored at high pH and hydrogen peroxide oxidation is favored at low pH. Just the opposite is true when employing $(1)Fe^{III}(X)$ (X = H_2O, HO^-). These results are discussed.

Catalase enzymes are present in most aerobic forms of life and are responsible for the decomposition of hydrogen peroxide to molecular oxygen and water (eq 1). They are usually tetrameric,

$$2H_2O_2 \rightarrow 2H_2O + O_2 \quad (1)$$

consisting of identical subunits each associated with one iron(III) protoporphyrin IX cofactor. The three-dimensional structures of the enzymes from a fungus and beef liver have been determined.[1] The axial ligand distal to the reactive face of the iron(III) porphyrin moiety is a tyrosine hydroxyl group of the apoenzyme, and adjacent to the reactiver face there is found a histidine imidazole function. The role of the latter is believed to be that of a general-base catalyst. It is thought that nondissociated hydrogen peroxide is the reactant in the first step.[2-4]

The higher valent iron–oxo species of catalase[2a,5-7] (much like horseradish peroxidase) are referred to as compounds I and II. Compound I represents an iron(IV)–oxo porphyrin π-cation radical $[(^{+\bullet}Porph)(TyrO)Fe^{IV}O]$, while compound II is an iron(IV)–oxo–porphyrin ($(Porph)(TyrO)Fe^{IV}O$).[7,8] The compound I state is generated on reaction of catalase with hydrogen peroxide, and

Chart I

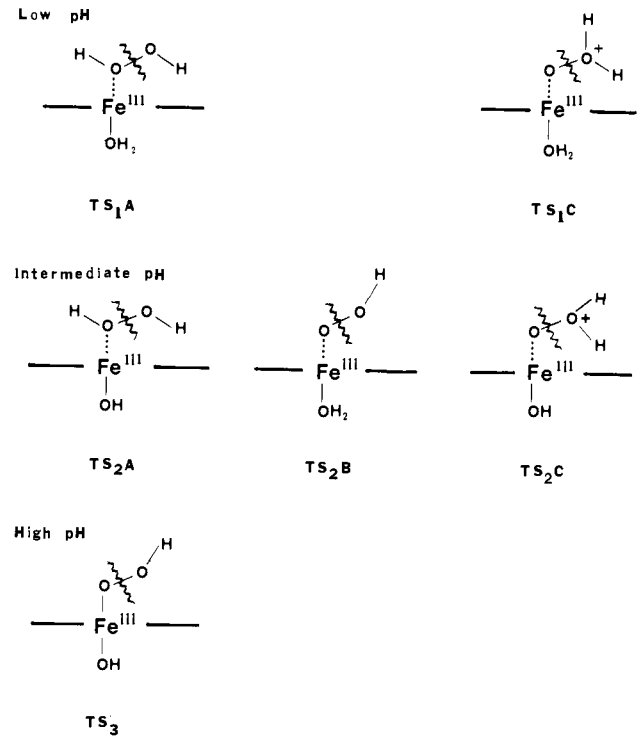

it returns to the iron(III) state on reaction with a second hydrogen peroxide molecule (eq 2). The first step is rate determining.[9]

$$(Porph)(TyrO)Fe^{III} + H_2O_2 \rightarrow (^{+\bullet}Porph)(TyrO)Fe^{IV}O + H_2O \quad (2)$$

$$(^{+\bullet}Porph)(TyrO)Fe^{IV}O + H_2O_2 \rightarrow (Porph)(TyrO)Fe^{III} + H_2O + O_2$$

(1) (a) Fita, I.; Rossmann, M. G. *J. Mol. Biol.* **1986**, *188*, 49. (b) Fita, I.; Rossmann, M. G. *J. Mol. Biol.* **1985**, *185*, 21. (c) Murthy, M. R. N.; Reid, T. J.; Siciganano, A.; Tanaka, N.; Rossmann, M. G. *J. Mol. Catal.* **1981**, *15*, 465.

(2) (a) Schonbaum, G. R.; Chance, B. In *The Enzymes*, 3rd ed.; Boyer, P. D., Ed.; Academic: New York, 1976; Vol. 13, p 363. (b) Chance, B. *J. Biol. Chem.* **1952**, *194*, 471. (c) Chance, B. *J. Biol. Chem.* **1950**, *182*, 649. (d) Jones, P.; Suggett, A. *Biochem. J.* **1968**, *110*, 617.

(3) Ogura, Y. *Arch. Biochem. Biophys.* **1955**, *57*, 288.

(4) Palcic, M. M.; Dunford, H. B. *J. Biol. Chem.* **1980**, *255*, 6128.

(5) (a) Deisseroth, A.; Dounce, A. *Physiol. Rev.* **1970**, *50*, 319. (b) Frew, J. E.; Jones, P. In *Advances in Inorganic and Bioinorganic Mechanisms*; Sykes, A. G., Ed.; Academic: New York, 1984, Vol. 3, p 175.

(6) Traylor, T. G.; Lee, W. A.; Stynes, D. V. *J. Am. Chem. Soc.* **1984**, *106*, 755.

(7) Hanson, L. K.; Chang, C. K.; Davis, M. S.; Fajer, J. *J. Am. Chem. Soc.* **1981**, *103*, 663.

(8) Hashimoto, S.; Tatsuno, Y.; Kitagawa, T. *Proc. Natl. Acad. Sci. U. S.A.* **1986**, *83*, 2417.

0002-7863/87/1509-7865$01.50/0

Chart II

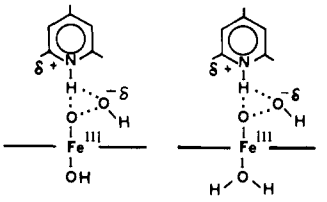

TS_2A_{gb} TS_2C_{ga}

In a recent study[10] we described the reaction of hydrogen peroxide with [5,10,15,20-tetrakis(2,6-dimethyl-3-sulfonatophenyl)porphinato]iron(III) [(**1**)Fe^{III}(X), where X = H_2O and HO^-]. (**1**)Fe^{III}(X) is water soluble and sterically blocked to μ-oxo

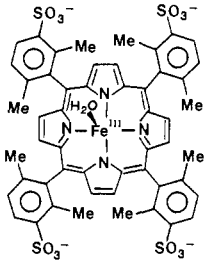

(**1**)$Fe^{III}(H_2O)$

dimer formation and stacking. The distal axial ligand (X) is an oxygen, much as in the case of catalase. From the pH dependence of the reaction of (**1**)Fe^{III}(X) with hydrogen peroxide there could be identified three transition-state compositions that give rise to the compound I oxidation state. Transition-state cartoons are provided in Chart I. The alternate cartoons at low and intermediate pH are allowable, since they are kinetically equivalent and kinetically competent. Transition-state structures TS_1C and TS_2C involve the generation of iron(IV)–oxo porphyrin π-cation radical with release of water as leaving group and as such must represent heterolytic hydroperoxide O–O bond cleavage. Transition-state structures TS_1A, TS_2A, TS_2B, and TS_3 could lead to higher valent iron–oxo porphyrin species by either heterolytic or a stepwise mechanism involving homolytic O–O bond scission. Oxyanion bases do not exhibit a catalytic effect upon the rate-determining step of formation of ($^{+\bullet}$**1**)Fe^{IV}O-ligated species. The single nitrogen base that was investigated (2,4,6-collidine) exhibited easily measurable catalysis at low and intermediate pH values. The transition-state cartoons of Chart II are kinetically competent and reasonable. The cartoons TS_2A_{gb} and TS_2C_{ga} represent catalysis by the nitrogen base of proton transfer to the leaving oxygen, so that the reactions occur by O–O heterolysis with water as the leaving group. Catalysis by the nitrogen base and lack of catalysis by oxyanion bases may be due to the favorable electrostatic interactions in the transition state for the former.

We report here results of the investigation of (**1**)Mn^{III}(X) (X = H_2O, HO^-) with hydrogen peroxide. Particular attention is given to the determination of (i) the dependence of composition of the critical transition states upon pH, (ii) the influence of general-acid and general-base species upon rate, and (iii) the influence of pH on competitive rates for oxidation of hydrogen peroxide species and 1e-transfer oxidations.

Experimental Section

Materials. Deionized, doubly distilled water was used throughout the study. The diammonium salt of 2,2′-azinobis(3-ethylbenzthiazoline-sulfonic acid) (ABTS) was purchased from Sigma Chemicals Co. and was used as received. 2,4,6-Collidine (Sigma) was shown to be 100% pure by gas chromatography. All the buffer and salt solutions were prepared from reagent-grade chemicals and passed through a Chelex 100 column to remove possible heavy-metal contaminations. The cuvettes were regularly soaked in 1% EDTA solution overnight and washed thoroughly with doubly distilled water. Hydrogen peroxide solutions were prepared by dilution of Mallinckrodt reagent-grade 30% hydrogen peroxide and stored at 4 °C prior to use. The concentration of hydrogen peroxide in these solutions was periodically determined by titration with potassium permanganate.[11] Imidazole (ImH) was bought from Aldrich Chemical Co. and was twice recrystallized from benzene prior to kinetic studies.

5,10,15,20-Tetrakis(2,6-dimethyl-3-sulfonatophenyl)porphyrin (1) was synthesized as reported previously.[10]

[5,10,15,20-Tetrakis(2,6-dimethyl-3-sulfonatophenyl)porphinato]manganese(III) hydroxide [(**1**)Mn^{III}(OH)] was synthesized by a modified procedure[12] as follows: **1** (80 mg, 0.06 mmol) and $Mn(OAc)_2 \cdot 4H_2O$ (200 mg, 0.82 mmol) in 15 mL of water were heated at 85 °C for 6 h. The reaction was monitored by recording the UV–vis spectra (Soret region) of the reaction mixture. After the reaction was complete, the solution was reduced to 5 mL by rotoevaporation and passed through a Dowex 50WX-8 (H^+ form) cation-exchange resin column to remove the excess Mn^{2+} ions. The eluate, containing the manganese(III) porphyrin, was collected, reduced to 3 mL, and taken to pH 8 with 0.1 M NaOH prior to rotoevaporation to dryness. After the solid material was dissolved in 2 mL of methanol, it was chromatographed on a Sephadex LH 20 column with methanol as the eluent. One purple band developed and was collected. Evaporation of the solvent afforded 70 mg (90%) of a dark purple material: ^{1}H NMR (300 MHz, D_2O) δ 8.1, 6.7 (br s, Ph H), 3.3 (br s, o-CH_3), −30 (br s, half-width 1200 Hz, β-pyrrole H); UV–vis (pH 7.0) 598 nm (ϵ 6370), 565 (11 320), 466 (104 900), 413 (sh, 37 960), 398 (500), 376 (50 140); R_f [KC_{18} plates (Whatman), n-butanol:water (2% tetrabutylammonium bromide) = 8:20] 0.86, 0.53 (most abundant), 0.33. Anal. Calcd for $(C_{52}H_{40}N_4S_4O_{12}Na_4)Mn(OH)\cdot 11H_2O$ (FW 1403.15): C, 44.51; H, 4.52; N, 3.99; Na, 6.55; Mn, 3.91; S, 9.14. Found: C, 44.5; H, 4.48; N, 3.81; Mn, 3.76; Na, 7.51; S, 8.28.

Instrumentation. UV–vis spectral measurements were carried out with a Cary 118C spectrophotometer at 30 °C. ^{1}H NMR spectra were recorded on a Nicolet NT-300 spectrometer (300 MHz). Chemical shifts are reported (δ) downfield from tetramethylsilane (external standard). Elemental analysis was carried out by Galbraith Laboratories, Inc., Knoxville, TN. For reversed-phase thin-layer chromatography, KC_{18} plates were used. Measurements of pH were carried out with a Radiometer Model pH M26 with Metrohm electrode. Spectrophotometric pK_a determinations as well as determinations of equilibrium constants for imidazole ligation were carried out at 30 °C on a Cary 118C spectrophotometer equipped with a thermostated cell (path length 10 mm), fitted with a glass electrode. Kinetic traces were recorded on a Perkin-Elmer fast-scanning spectrophotometer, Model 553, having a constant-temperature cell holder. Rapid reactions were followed with a Durrum stopped-flow spectrophotometer thermostated at 30 °C interfaced to a Zenith computer equipped with OLIS data acquisition and processing software (On-Line Instruments Systems, Inc.). A Hewlett-Packard 9825A computer, equipped with a 9864A digitizer and plotter, was employed for the analysis of pseudo-first-order kinetic traces, titration curves, and pH–rate profiles, with the appropriate software programs written for these purposes. Oxygen evolution studies were carried out with oxygen electrodes (5331) and YSI oxygen meter (Model 53, Yellow Springs Instrument Co., Inc.).

Kinetic Studies. Phosphate and carbonate buffers were prepared by mixing solutions of known concentrations of Na_2HPO_4/NaH_2PO_4 and $NaHCO_3/Na_2CO_3$, whereas 2,4,6-collidine/collidine hydrochloride buffer was prepared by mixing 2,4,6-collidine in MeOH with sufficient concentrations of dilute HCl to yield the desired pH. It should be noted that for reactions with collidine buffer there is a change in solvent composition from water to 10% MeOH in H_2O. Stock solutions of manganese(III) porphyrin were prepared in the appropriate buffers and stored in blackened glass containers at 3–5 °C. Reactions were initiated by mixing 0.05 mL of 5.0×10^{-3} M H_2O_2 solution (added with syringe) and a buffered manganese(III) porphyrin solution, containing ABTS and sodium nitrate (for ionic strength adjustment to 0.23 M). The pH of the reaction mixture was checked to be within ±0.04 pH unit before and after the completion of each kinetic run. Rapid reactions (at pH >11.0) were carried out by use of a stopped-flow spectrophotometer ($[(1)Mn^{III}]_i = 2.3 \times 10^{-6}$ M, $[H_2O_2]_i = 8.3 \times 10^{-5}$ M and $[ABTS]_i = 1.6 \times 10^{-3}$ M). The pseudo-first-order rate constants for the rapid reactions were determined from the analysis of absorbance vs time with a Zenith computer

(9) Walsh, C. In *Enzymatic Reaction Mechanisms*; Freeman: San Francisco, 1979.

(10) Zipplies, M. F.; Lee, W. A.; Bruice, T. C. *J. Am. Chem. Soc.* **1986**, *108*, 4433.

(11) (a) Simoyi, R. H.; DeKepper, P.; Epstein, I. R.; Kustin, K. *Inorg. Chem.* **1986**, *25*, 538. (b) Kolthoff, I. M.; Sandell, E. B.; Meehan, E. J.; Bruckenstein, S. In *Quantitative Chemical Analysis, 4th ed.*; Macmillan: London, 1969, p 834.

(12) Harriman, A.; Porter, G. *J. Chem. Soc. Faraday Trans. 2* **1979**, 1532.

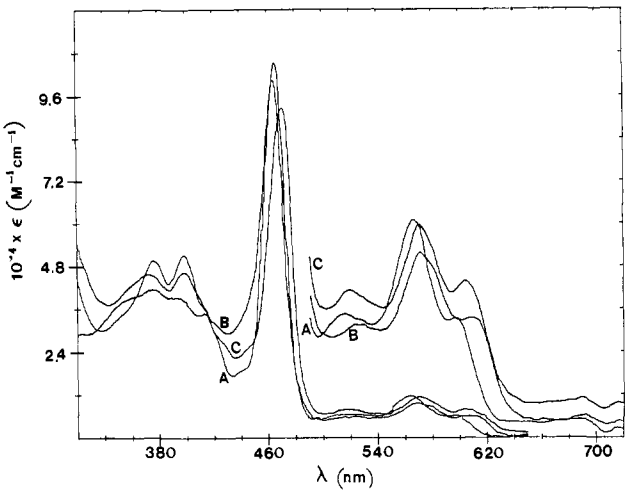

Figure 1. Visible absorption spectra of (1)$Mn^{III}X$. A corresponds to species (1)$Mn^{III}(H_2O)_2$ at pH 7.59 (phosphate buffer); B corresponds to species (1)$Mn^{III}(OH)_2$ (0.20 M KOH); and C is the spectrum for the species (1)Mn^{III}(ImH) at [ImH] = 0.12 M (phosphate buffer, pH 7.59). The spectra from 490 to 720 nm are magnified 5-fold.

equipped with OLIS data acquisition and processing software.

Results

The water-soluble manganese(III) porphyrin salt [5,10,15,20-tetrakis(2,6-dimethyl-3-sulfonatophenyl)porphinato]manganese(III) hydroxide ((1)Mn^{III}(OH)), prepared by heating 5,10,15,20-tetrakis(2,6-dimethyl-3-sulfonatophenyl)porphyrin (1) with an excess of manganese(II) acetate in water for 6 h, displayed three spots (of identical visible spectra) on a reversed-phase thin-layer chromatogram. One spot was found to be much more abundant than the other two. This observation shows that there are at least three of the possible four atropisomers of (1)Mn^{III}(OH) present.[10] The electronic absorption spectrum of (1)Mn^{III}(OH), at pH 7, is given in Figure 1A. The position of the Soret band (466 nm) and its molar extinction coefficient (ϵ 1.05×10^5 cm^{-1} M^{-1}) are comparable with that of [*meso*-tetrakis(4-sulfonatophenyl)porphinato]manganese(III).[12] The water-soluble (1)-Mn^{III}(OH) was further characterized by ^1H NMR spectroscopy in D_2O. The ^1H NMR spectrum shows a very broad signal at δ −30, which is characteristic of the β-pyrrole protons of manganese(III) porphyrins.[13]

Determination of the pK_a of (1)$Mn^{III}(H_2O)_2$ was carried out by spectrophotometric titration at 376, 398, 433, 565, and 613 nm (eq 3) between pH 3.5 and 13.2. The initial ionic strength was adjusted to μ = 1.0 by the addition of KNO_3. There could

$$(1)Mn^{III}(H_2O)_2 \overset{K_a}{\rightleftharpoons} (1)Mn^{III}(H_2O)(OH) + H^+ \quad (3)$$

not be observed any significant spectral changes from pH 3.5 to 11.0. The electronic spectrum changes markedly, after pH 11, (from dark red to green) with isosbestic points at 359, 420, 460, 481.5, 491.5, 578, 590, 603, and 645 nm (Figure 1B). The least-squares pK_a of 12.2 ± 0.15 was determined by the fitting of the change of absorbance with pH to a theoretical curve for the dissociation of a monoprotic acid. As in the case of (1)-$Fe^{III}(H_2O)_2$,[10] this observation clearly demonstrates that all the atropisomers of (1)$Mn^{III}(H_2O)_2$ possess indistinguishable pK_a values, showing that the electronic nature of the bound manganese(III) of each isomer is the same.

The equilibrium constant (K_1) for axial ligation with imidazole was determined by spectrophotometric titration with imidazole at constant pH values employing lutidine buffer (1.5×10^{-2} M). The concentration of the manganese(III) porphyrin was maintained at 1.5×10^{-4} M, whereas the ionic strength (1.0) was regulated with $NaClO_4$. Imidazole ligation (eq 4 and 5) is characterized by change of color from dark red (λ_{max} 376, 398, 466, 514, 566, and 598 nm, Figure 1A) to green (λ_{max} 373, 400, 472, 519, 570, and 605 nm, Figure 1C), with isosbestic points at 365, 420, 446, 468, 495, 575, 592, and 599 nm. No further

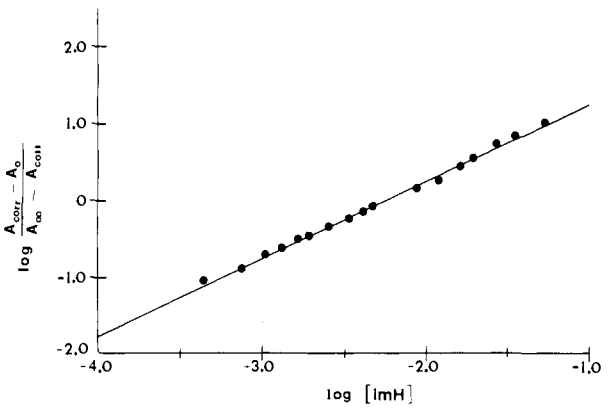

Figure 2. Plot of log $(A_{cor} - A_0)/(A_\infty - A_{cor})$ vs log [ImH] at 609 nm. The slope of 1.0 ± 0.1 establishes monoligation by ImH. The value of log K_1 is obtained from the intercept [30 °C, [(1)Mn^{III}(X)] = 1.50×10^{-4} M, pH 6.5 with lutidine buffer 1.5×10^{-2} M].

$$(1)Mn^{III}(H_2O)_2 + ImH \overset{K_1}{\rightleftharpoons} (1)Mn^{III}(H_2O)(ImH) \quad (4)$$

$$(1)Mn^{III}(H_2O)(ImH) + ImH \overset{K_2}{\rightleftharpoons} (1)Mn^{III}(ImH)_2 \quad (5)$$

change in absorbance was seen after reaching 0.1 M in imidazole concentration. The concentration of free imidazole ([ImH]) was calculated from the total imidazole concentration ([ImH_2^+] + [ImH]), the pK_a of imidazole (6.95),[14] and the pH of the solution. The binding constant (K_1) was calculated[15] from plots of log $((A_{cor} - A_0)/(A_\infty - A_{cor}))$ vs log [ImH] (Figure 2), where A_0 is the absorbance of the manganese(III) porphyrin in the absence of imidazole, A_{cor} is the absorbance at a particular imidazole concentration, and A_∞ is the absorbance in the presence of a large excess of imidazole. The slope of the straight line of Figure 2 is 1.0 ± 0.1, showing that only one ImH ligates to the manganese(III) porphyrin. The log of the equilibrium constant (log K_1) for ImH ligation was obtained from the intercept determined from the best fit of a line of slope 1.0. The determinations were carried out at two different wavelengths (565 and 609 nm) at pH values 6.5, 7.2, and 7.5. The average value of log K_1 is 2.20 ± 0.05.

The kinetics of the reaction of the manganese(III) porphyrin with hydrogen peroxide, in aqueous medium, were followed by the use of 2,2′-azinobis(3-ethylbenzthiazolinesulfonic acid) (ABTS) as an easily oxidizable substrate to partially trap the reactive higher valent manganese–oxo porphyrin species.[16] One-electron oxidation of ABTS provides the bluish green radical cation $ABTS^{\bullet+}$, which can be conveniently followed at 660 nm. Reactions were carried out under the pseudo-first-order conditions of $[(1)Mn^{III}]_i < [H_2O_2]_i \ll [ABTS]_i$. Sufficient ABTS was employed to prevent oxidation of $ABTS^{\bullet+}$ to form the $ABTS^{2+}$ dication.[17] All kinetic traces were found to follow the first-order rate law under the conditions reported herein. The reaction was studied in the range pH 7.5–12.0, and the ionic strength (μ = 0.23) was maintained with $NaNO_3$ in order that the present system may be compared with the reaction of H_2O_2 with the corresponding iron(III) porphyrin.[10] The oxidation products were found to be $ABTS^{\bullet+}$ and molecular oxygen.

Dependence of the rate of $ABTS^{\bullet+}$ formation upon the concentration (1.0×10^{-6}–1.0×10^{-5} M) of manganese(III) porphyrin was determined at pH 7.59 (N_2 atmosphere) and constant [ImH]

(13) Hansen, A. P.; Goff, H. M. *Inorg. Chem.* **1984**, *23*, 4519.

(14) Weast, R. C., Ed. In *Handbook of Chemistry and Physics*; CRC: Cleveland, 1971; p D118.

(15) Walker, F. A.; Lo, M.-W.; Ree, M. T. *J. Am. Chem. Soc.* **1976**, *98*, 5552.

(16) (a) Huenig, S.; Balli, H.; Conrad, H.; Schott, A. *Justus Liebigs Ann. Chem.* **1964**, *676*, 32, 36, 52. (b) Grawehn, K.; Weilinger, H.; Werner, W. *Fresenius Z. Anal. Chem.* **1970**, *252*, 222. (c) Werner, W.; Rey, H.-G.; Wielinger, H. *Fresenius Z. Anal. Chem.* **1970**, *252*, 224. (d) Puetter, J.; Becker, R.; In *Methods of Enzymatic Analysis*, 3rd ed.; Bergmeyer, H. V., Ed.; Verlag Chemie: Weinheim, 1983; Vol. 3, p 286.

(17) Gallati, H. *J. Clin. Biochem.* **1976**, *17*, 1.

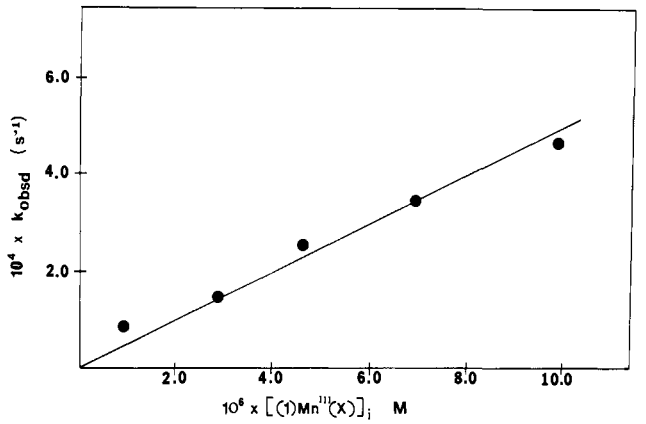

Figure 3. Plot of the pseudo-first-order rate constants (k_{obsd}) for the formation of $ABTS^{\bullet+}$ vs $[(\mathbf{1})Mn^{III}(X)]_i$ [$[ABTS]_i = 1.0 \times 10^{-2}$ M, $[H_2O_2]_i = 8.3 \times 10^{-5}$ M, pH 7.59 (0.058 M phosphate buffer), $\mu = 0.23$ M].

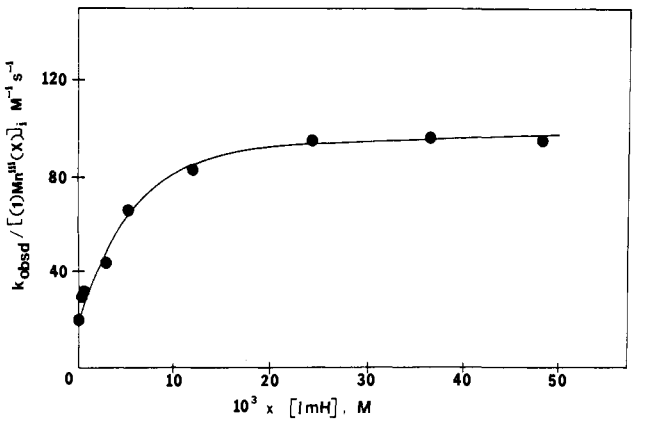

Figure 4. Plot of the apparent second-order rate constant k_{1y} vs [ImH] [$[(\mathbf{1})Mn^{III}(X)]_i = 4.6 \times 10^{-6}$ M, $[H_2O_2]_i = 1.67 \times 10^{-4}$ M, $[ABTS]_i = 1.0 \times 10^{-2}$ M, pH 7.59 (0.058 M, phosphate buffer), $\mu = 0.23$ M]. The limiting value at high $[ImH]_i$ is equal to the apparent second-order rate constant (k_b) for the oxidation of $(\mathbf{1})Mn^{III}(ImH)(X)$ by hydrogen peroxide species.

(5.3×10^{-3} M), $[H_2O_2]$ (8.3×10^{-5} or 1.67×10^{-4} M), and [ABTS] (1.0×10^{-2} M). Since the pseudo-first-order rate constant, k_{obsd}, increases linearly over a 10-fold increase in manganese(III) porphyrin (Figure 3), the reaction is first order in this catalyst. The presence of oxygen was found to have no influence on k_{obsd}.

Dependence of the pseudo-first-order rate of O_2 formation upon the concentration of manganese(III) porphyrin was determined over a 10-fold range of the catalyst concentration. Values of the manganese(III) porphyrin concentrations and the corresponding values of k_{obsd} follow: 9.4×10^{-7} M, 1.10×10^{-4} s^{-1}; 2.94×10^{-6} M, 8.7×10^{-5} s^{-1}; 4.64×10^{-6} M, 2.0×10^{-4} s^{-1}; 7.1×10^{-6} M, 4.2×10^{-4} s^{-1}; 1.0×10^{-5} M, 6.0×10^{-4} s^{-1}. The second-order rate constant calculated from the linear plot of k_{obsd} vs [catalyst] is indistinguishable (44.8 $M^{-1} s^{-1}$) from that determined (48.6 $M^{-1} s^{-1}$) for the formation of $ABTS^{\bullet+}$ under conditions of similar concentrations and pH.

The values of k_{obsd} for $ABTS^{\bullet+}$ formation (pH 7.59) are independent of the concentration of H_2O_2 (4.2×10^{-5}–1.67×10^{-4} M) at constant [manganese(III) porphyrin], [ImH], and [ABTS] (Table I). For a catalyzed reaction, under conditions of nonsaturation of catalyst, k_{obsd} is independent of substrate concentrations so that the reaction is first order in hydrogen peroxide.[18]

Independence of the reaction rate on the concentration of ABTS was shown by varying $[ABTS]_i$ over a 10-fold concentration range

Table I. Independence of k_{obsd} on the Initial Concentration of H_2O_2 at Constant $[(\mathbf{1})Mn^{III}]_i$ (4.6×10^{-6} M), $[ImH]_i$ (5.3×10^{-3} M), $[ABTS]_i$ (1.0×10^{-2} M), and pH (7.59)

$10^5[H_2O_2]_i$, M	$10^4 k_{obsd}$, s^{-1}	$10^5[H_2O_2]_i$, M	$10^4 k_{obsd}$, s^{-1}
4.2	2.6	12.5	2.7
8.3	2.5	16.7	2.9

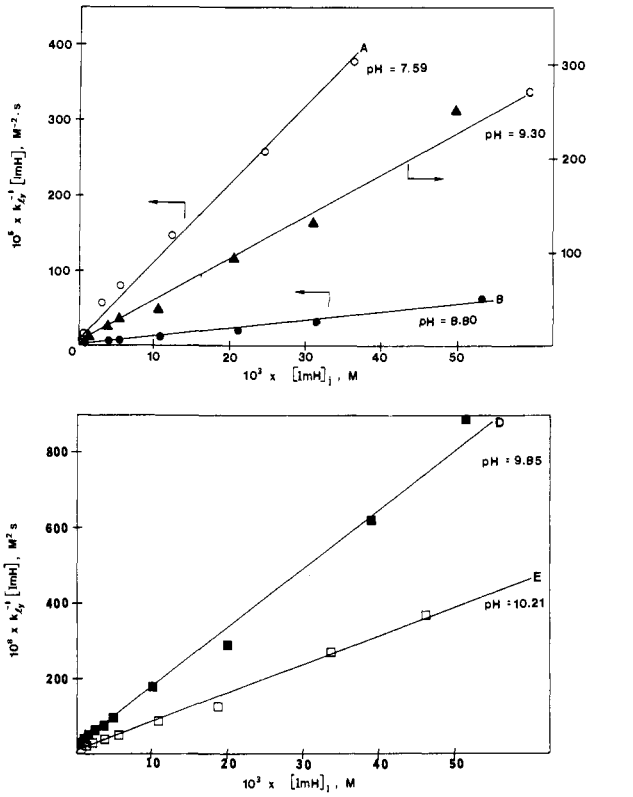

Figure 5. Plots of $(1/k_{1y})$[ImH] vs [ImH] at different pH values: line A, pH 7.59 (0.058 M phosphate buffer); line B, pH 8.90 (0.165 M HCO_3^-/CO_3^{2-} buffer); line C, pH 9.30 (0.133 M HCO_3^-/CO_3^{2-} buffer); line D, pH 9.85 (0.08 M HCO_3^-/CO_3^{2-} buffer); line E, pH 10.21 (0.071 M HCO_3^-/CO_3^{2-} buffer).

while holding $[(\mathbf{1})Mn^{III}]_i$ (4.6×10^{-6} M), $[H_2O_2]_i$ (8.3×10^{-5} M), $[ImH]_i$ (5.1×10^{-3} M), and the pH (7.59) constant. The values of k_{obsd} were found to be 2.5×10^{-4}, 2.3×10^{-4}, 2.3×10^{-4}, 2.6×10^{-4}, and 2.5×10^{-4} s^{-1} with $[ABTS]_i$ at 1.0×10^{-2}, 7.9×10^{-3}, 6.5×10^{-3}, 2.7×10^{-3}, and 9.3×10^{-4} M, respectively. Thus, formation of $ABTS^{\bullet+}$ is zero order in $[ABTS]_i$.

Dependence of the reaction rate on the concentration of ImH was studied at five pH values from 7.59 to 10.21 at constant $[(\mathbf{1})Mn^{III}]_i$, $[H_2O_2]_i$, and $[ABTS]_i$. In Figure 4 the second-order rate constant determined at pH 7.59 (k_{1y}, eq 6) is plotted vs $[imidazole]_i$. Such plots have nonzero intercepts, and the rate

$$\frac{d[ABTS^{\bullet+}]}{dt} = \frac{-d[H_2O_2]}{dt} = k_{1y}[(\mathbf{1})Mn^{III}][H_2O_2] \quad (6)$$

$$k_{obsd} = k_{1y}[(\mathbf{1})Mn^{III}]_i$$

$$k_{1y} = \frac{A + B[ImH]}{1 + K_1[ImH]} \quad (7)$$

constants reach limiting values with increase in imidazole concentration. The dependence of k_{1y} (eq 6) upon $[ImH]_i$ may be analyzed by the use of eq 7,[19] where A is the rate constant for the manganese(III) porphyrin not ligated to ImH and B is the product of the equilibrium constant for ImH monoligation (K_1) and the rate constant (k_b) for the reaction of the imidazole-ligated

(18) (a) Dicken, C. M.; Lu, F.-L.; Nee, M. W.; Bruice, T. C. *J. Am. Chem. Soc.* **1985**, *107*, 5776. (b) Balasubramanian, P. N.; Sinha, A.; Bruice, T. C. *J. Am. Chem. Soc.* **1987**, *109*, 1456.

(19) Cannon, R. D. In *Electron Transfer Reactions*; Butterworths: Boston, 1980; p 108.

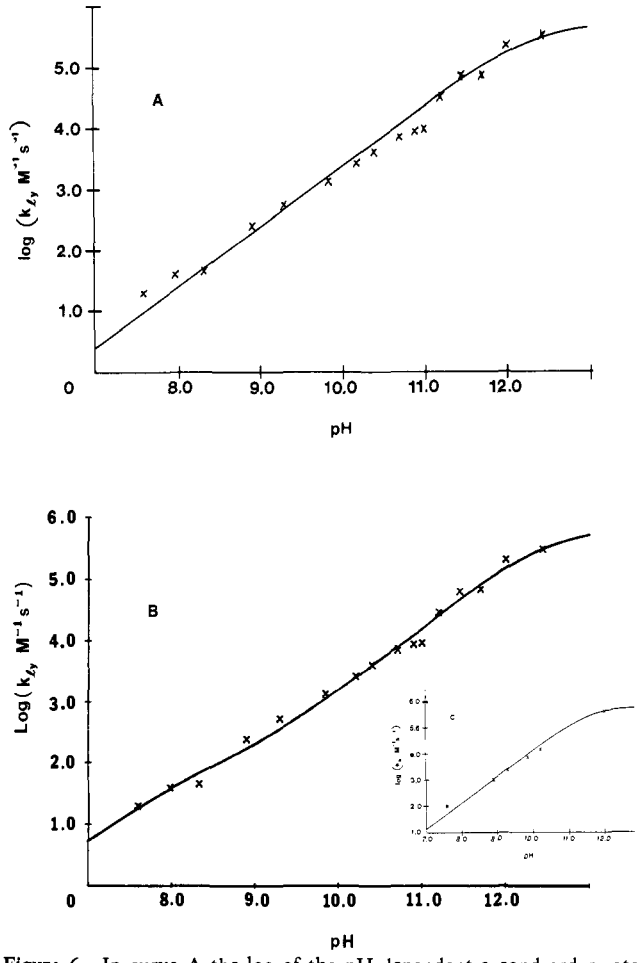

Figure 6. In curve A the log of the pH-dependent second-order rate constant k_{1y} is plotted vs pH for the reaction of (**1**)Mn^{III}(X) with hydrogen peroxide species. The points are experimentally determined rates for $ABTS^{\bullet+}$ formation and the line generated from eq 12 (30 °C, μ = 0.23 M). Curve B corresponds to a fit of the same experimental points with a line generated from eq 13. The inset to the figure represents a plot of the log of the apparent second-order rate constant (k_b) for the reaction of (**1**)Mn^{III}(ImH)(X) with hydrogen peroxide species vs pH (30 °C, μ = 0.23 M).

manganese(III) porphyrin. Rearrangement of eq 7 provides eq 8. The equilibrium constant K_1 may be calculated from the ratio

$$(1/k_{1y})[\mathrm{ImH}] = \frac{1}{a[\mathrm{ImH}]^{-1} + b} + \frac{K_1[\mathrm{ImH}]}{a[\mathrm{ImH}]^{-1} + b} \quad (8)$$

(slope/intercept) of plots of $(1/k_{1y})$[ImH] vs [ImH] (Figure 5). Determined log K_1 values (at μ = 0.23) are as follows: 2.80, pH 7.60; 2.99, pH 8.90; 2.94, pH 9.3; 2.90, pH 9.85; and 2.90, pH 10.21—average value 2.90 ± 0.05. The latter may be compared with the value of 2.20 ± 0.05 (at μ = 1.0) determined by spectrophotometric titration. In accordance with the above analysis the rate law for the oxidation reaction, in the presence of ImH, may be written as in eq 9 from which there follows eq 10 and 11. The rate constants k_b were calculated at given pH values (7.6–10.2) as the limiting values (as in Figure 4) at high [ImH] in plots of k_{1y} vs [ImH] (eq 7). The determined values of k_b are shown in the plot of the inset to Figure 6B.

$$\text{rate} = k_a[(\mathbf{1})\mathrm{Mn^{III}(H_2O)_2}][\mathrm{H_2O_2}] + k_b[(\mathbf{1})\mathrm{Mn^{III}(ImH)(H_2O)}][\mathrm{H_2O_2}] \quad (9)$$

$$\frac{-\mathrm{d}[\mathrm{H_2O_2}]}{\mathrm{d}t} = \frac{(k_a + k_bK_1[\mathrm{ImH}])[(\mathbf{1})\mathrm{Mn^{III}}]_{\mathrm{total}}[\mathrm{H_2O_2}]}{1 + K_1[\mathrm{ImH}]} \quad (10)$$

$$k_{\mathrm{obsd}}/[(\mathbf{1})\mathrm{Mn^{III}}]_{\mathrm{total}} = k_{1y} = \frac{k_a + k_bK_1[\mathrm{ImH}]}{1 + K_1[\mathrm{ImH}]} \quad (11)$$

Table II. Effect of Various Concentrations of Collidine Buffer on k_{obsd} at pH 8.34 ([(**1**)Mn^{III}] = 4.65 × 10^{-6} M, [H_2O_2] = 8.3 × 10^{-5} M, and [ABTS] = 1.0^{-2} M)

$10^3[B]_T$, M	10^4k_{obsd}, s^{-1}	$10^3[B]_T$, M	10^4k_{obsd}, s^{-1}
1.22	1.75	20.0	2.62
4.10	1.60	41.0	1.94
8.10	2.40		

Dependence of the reaction rate upon pH and the concentration of buffer species was investigated with $H_2PO_4^-/HPO_4^{2-}$, HCO_3^-/CO_3^{2-}, 2,4,6-collidine hydrochloride/2,4,6-collidine, and H_2O/HO^- buffers to regulate the pH in the range 7.5–12.0. With [manganese(III) porphyrin]$_i$ = 4.6 × 10^{-6} M, [H_2O_2]$_i$ = 8.3 × 10^{-5} M, and [ABTS]$_i$ = 1.0 × 10^{-2} M, in no case could catalysis be detected. Buffer dilutions with 2,4,6-collidine/2,4,6-collidine hydrochloride (pH 8.34) were carried out from 1.2 × 10^{-3} to 4.0 × 10^{-2} M (33-fold variation) as shown in Table II.

In the log k_{1y} vs pH profile of Figure 6A the points are experimental, and the line was generated (standard error 1.83 × 10^{-1}) from the empirical eq 12. The kinetic parameters calculated

$$k_{1y} = \frac{k_2K_0a_H}{(K_c + a_H)(K_0 + a_H)} + \frac{k_3K_cK_0}{(K_c + a_H)(K_0 + a_H)} \quad (12)$$

from the fitting are k_2 = 8.93 × 10^4 M^{-1} s^{-1}, k_3 = 4.83 × 10^5 M^{-1} s^{-1}, K_c = 3.71 × 10^{-13} M^{-1}, and K_0 = 2.45 × 10^{-12} M^{-1}. The kinetic data are better fit (standard error 1.17 × 10^{-1}; Figure 6B) to the empirical eq 13. The values of the constants used for fitting are

$$k_{1y} = \left(\frac{k_2K_da_H}{K_dK_e + K_da_H + a_H^2}\right)\left(\frac{a_H}{K_0 + a_H}\right) + \left(\frac{k_3K_da_H}{K_dK_e + K_da_H + a_H^2}\right)\left(\frac{K_0}{K_0 + a_H}\right) + \left(\frac{k_4K_dK_e}{K_dK_e + K_da_H + a_H^2}\right)\left(\frac{K_0}{K_0 + a_H}\right) \quad (13)$$

as follows: k_2 = 87.6 M^{-1} s^{-1}, k_3 = 5.38 × 10^4 M^{-1} s^{-1}, k_4 = 6.94 × 10^5 M^{-1} s^{-1}, K_d = 6.33 × 10^{-9} M^{-1}, K_e = 3.22 × 10^{-13} M^{-1}, and K_0 = 2.82 × 10^{-12} M^{-1}. It should be mentioned that the reaction rate and yield of $ABTS^{\bullet+}$ are very small below pH 7.59.

Yields of the Products $ABTS^{\bullet+}$ and O_2. The yield of $ABTS^{\bullet+}$ was determined for each kinetic run. It should be noted that one H_2O_2 molecule gives rise to two $ABTS^{\bullet+}$ radical species (eq 14).

$$\mathrm{H_2O_2} + 2\mathrm{ABTS} \rightarrow 2\mathrm{ABTS^{\bullet+}} + 2\mathrm{HO^-} \quad (14)$$

The combined yield of $ABTS^{\bullet+}$ plus O_2 equals 100% based on the concentration of H_2O_2 employed. In the absence of imidazole, at pH 7.59, the yield of $ABTS^{\bullet+}$ is 3.9%, while the yield of O_2 is 88%. Thus, H_2O_2 and ABTS compete as substrates for the reactive higher valence manganese–oxo porphyrin intermediate. This is also shown by the finding that the rates of formation of $ABTS^{\bullet+}$ and O_2 are comparable. At pH 7.59, k_{obsd} values for the formation of O_2 and $ABTS^{\bullet+}$ were determined to be 1.05 × 10^{-4} and 0.98 × 10^{-4} s^{-1}, respectively ([(**1**)Mn^{III}] = 4.6 × 10^{-6} M, [H_2O_2] = 1.67 × 10^{-4} M, [ABTS] = 1.0 × 10^{-2} M).

Upon addition of imidazole, at pH 7.59, there is a significant change in the yield of $ABTS^{\bullet+}$ (Table III). The yield of $ABTS^{\bullet+}$ increases from 3.9% to 40.0% for an increase in concentration of imidazole from 2.55 × 10^{-4} to 4.83 × 10^{-2} M (the highest [ImH]$_i$). Material balance was assessed at an imidazole concentration of 5.3 × 10^{-3} M. The yield of O_2 and $ABTS^{\bullet+}$ were determined to be 58% and 40%, respectively.

Dependence of the yields of O_2 and $ABTS^{\bullet+}$ products on the concentration of manganese(III) porphyrin was determined at constant [H_2O_2] = 8.3 × 10^{-5} M, [ImH] = 5.3 × 10^{-3} M, [ABTS] = 1.0 × 10^{-2} M, and [phosphate buffer]$_T$ = 0.058 M (pH 7.59) (Table IV). Inspection of Table IV shows that the yield of $ABTS^{\bullet+}$ increases from 20%, becoming constant at 50% as the

Table III. Dependence of the Yield of $ABTS^{\bullet+}$ on the Concentration of ImH at Constant $[(1)Mn^{III}]_i = 4.6 \times 10^{-6}$ M, $[H_2O_2]_i = 1.67 \times 10^{-4}$ M, $[ABTS]_i = 1.0 \times 10^{-2}$ M, pH 7.59, $[B]_T = 0.058$ M (Na_2HPO_4/NaH_2PO_4), and $\mu = 0.23$

$[ImH]_i$, M	$[ABTS^{\bullet+}]$, M (% yield)	$[ImH]_i$, M	$[ABTS^{\bullet+}]$, M (% yield)
0	1.28×10^{-5} (3.9)[a]	1.20×10^{-2}	1.39×10^{-4} (41.0)
2.55×10^{-4}	3.25×10^{-5} (9.7)	2.40×10^{-2}	1.35×10^{-4} (40.8)
5.10×10^{-4}	4.70×10^{-5} (14.0)	3.6×10^{-2}	1.36×10^{-4} (41.0)
2.65×10^{-3}	1.10×10^{-4} (33.7)	4.83×10^{-2}	1.31×10^{-4} (39.6)
5.30×10^{-3}	1.40×10^{-4} (41.0)[b]		

[a] The concentration of O_2 evolved was determined to be 7.0×10^{-5} M in an independent experiment, and the yield is 88%. [b] The concentration of O_2 evolved is 4.6×10^{-5} M (58.0%).

Table IV. Dependence of Product Yields on $[(1)Mn^{III}]_i$ at constant $[ImH]_i = 5.3 \times 10^{-3}$ M, $[H_2O_2]_i = 8.3 \times 10^{-5}$ M, $[ABTS]_i = 1.0 \times 10^{-2}$ M, pH 7.59, $[B]_T = 0.058$ M (Na_2HPO_4/NaH_2PO_4), and $\mu = 0.23$ M ($NaNO_3$)

$[catalyst]_i$, M	$10^5[ABTS^{\bullet+}]$, M (% yield)	$10^5[O_2]$, M (% yield)	total % yield
0.97×10^{-6}	3.3 (20)	2.9 (70)	90
2.90×10^{-6}	5.97 (36)	2.3 (55)	91
4.6×10^{-6}	7.0 (42)	2.6 (62)	104
7.15×10^{-6}	8.35 (50)	2.2 (52)	102
1.00×10^{-5}	8.98 (52)	1.9 (46)	98

Table V. Dependence of Product Yields on $[H_2O_2]_i$ and $[ABTS]_i$ at constant $[(1)Mn^{III}]_i = 4.60 \times 10^{-6}$ M, $[ImH]_i = 5.30 \times 10^{-3}$ M, pH 7.59, $[B]_T = 0.058$ M (Na_2HPO_4/NaH_2PO_4), $\mu = 0.23$ M ($NaNO_3$), and $T = 30$ °C

$[H_2O_2]_i$, M	$[ABTS]_i$, M	$[ABTS^{\bullet+}]$, M (% yield)	$10^5[O_2]$, M (% yield)
4.2×10^{-5}	1.0×10^{-2}	3.6×10^{-5} (44.2)	
8.30×10^{-5}	1.0×10^{-2}	7.0×10^{-5} (42.1)	2.6 (62)
1.25×10^{-4}	1.0×10^{-2}	1.0×10^{-4} (41.0)	
1.67×10^{-4}	1.0×10^{-2}	1.2×10^{-4} (37.0)	4.6 (58)
8.30×10^{-5}	7.0×10^{-3}	6.9×10^{-5} (41.4)	
8.30×10^{-5}	6.5×10^{-3}	7.0×10^{-5} (42.0)	
8.30×10^{-5}	2.7×10^{-3}	7.1×10^{-5} (43.0)	
8.30×10^{-5}	9.3×10^{-4}	6.3×10^{-5} (37.4)	

Table VI. Percentage Yields of $ABTS^{\bullet+}$ (Based on Hydrogen Peroxide Consumed) as a Function of pH for the Reaction of $(1)Mn^{III}(X)$ (4.6×10^{-6} M) with $[Hydrogen\ Peroxide]_T$ (8.3×10^{-5} M) ($[ABTS]_i = 1.0 \times 10^{-2}$ M)

pH	$ABTS^{\bullet+}$ yield, %	pH	$ABTS^{\bullet+}$ yield, %	pH	$ABTS^{\bullet+}$ yield, %
7.59	3.90	9.85	22.40	11.00	32.00
7.97	7.45	10.20	28.70	11.20	90.00
8.42	3.45	10.40	31.80	11.45	80.00
8.90	8.45	10.71	31.60	11.75	82.00
9.30	11.30	10.90	34.40		

concentration of manganese(III) porphyrin catalyst is increased, whereas the yield of O_2 decreases corresponding to account for the material balance.

Dependence of the yields of $ABTS^{\bullet+}$ and O_2 products upon $[H_2O_2]$ and [ABTS] is shown in Table V. From Table V the yield of $ABTS^{\bullet+}$ is nearly constant (40.0%) for different initial concentrations of H_2O_2, and the yield of O_2 under similar conditions is ~60.0%. Similarly, the yield of $ABTS^{\bullet+}$ at different concentrations of $[ABTS]_i$ is also a constant (40.0%) value.

pH Dependence of the Yields of O_2 and $ABTS^{\bullet+}$ in the Absence of ImH. The percent yield of $ABTS^{\bullet+}$ at constant [manganese(III) porphyrin], [ABTS], and $[H_2O_2]$ (Table VI) increases steadily from 4.0% (pH 7.59) to nearly 32.0% (pH 10.9) followed by a sharp increase to 89.0% (pH 11.2). Simultaneously, the yield of O_2 (pH 7.59, 88%; pH 10.2, 67.0%; pH 11.3, 14%) decreases correspondingly to preserve material balance. At pH 10.2, in the *absence* of ABTS ($[(1)Mn^{III}] = 4.64 \times 10^{-6}$ M, $[H_2O_2] = 8.3 \times 10^{-5}$ M), O_2 is formed in 100% yield. The value of k_{obsd} for O_2 formation (1.15×10^{-2} s^{-1}) may be compared with the k_{obsd} for $ABTS^{\bullet+}$ formation (1.22×10^{-2} s^{-1}) under the same conditions but in the presence of ABTS (1.0×10^{-2} M).

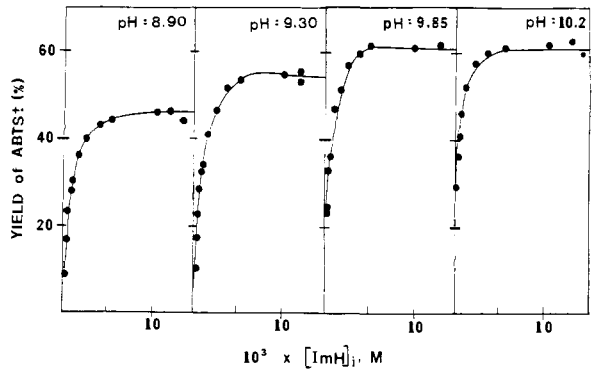

Figure 7. Plot of the percent yield of $ABTS^{\bullet+}$ vs $[ImH]_i$ at various pH values.

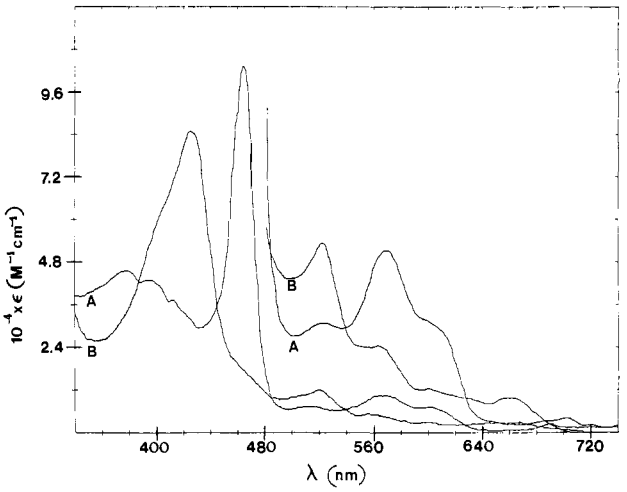

Figure 8. Visible absorption spectra of manganese species in the absence and presence of hydrogen peroxide species ($[(1)Mn^{III}(X)] = 4.60 \times 10^{-6}$ M, $[H_2O_2]_i = 8.3 \times 10^{-5}$ M, and [KOH] = 0.10 M (30 °C, $\mu = 0.20$ M). Spectrum A is that of $(1)Mn^{III}(HO)_2$. Spectrum B corresponds to the higher valent manganese–oxo species formed after addition of the hydrogen peroxide. The spectra from 490 to 720 nm are magnified by 5-fold.

Influence of Imidazole Ligation upon the Yield of $ABTS^{\bullet+}$ at Higher pH Values. The yield of $ABTS^{\bullet+}$ initially increases exponentially with an increase in $[ImH]_i$ (Figure 7), reaching a constant value at saturation of manganese(III) porphyrin. At pH >11.2, the yield of $ABTS^{\bullet+}$ reaches 100% when [ImH] is 0.025 M.

Formation of higher valent manganese–oxo species on reaction of manganese(III) porphyrin (4.6×10^{-6} M) with H_2O_2 (8.3×10^{-5} M) was studied by repetitive spectral scannning between 315 and 800 nm. At pH 7.60 [manganese(III) porphyrin] remained unaltered throughout the course of the reaction. At pH 10.2, however, the absorbance at the Soret peak of manganese(III) porphyrin (466 nm) decreases in concert with the formation of a manganese(IV)–oxo porphyrin (420 nm).[20] After all hydrogen peroxide has been consumed the manganese(IV)–oxo species decomposes over a ~24-h period to regenerate the original manganese(III) porphyrin species (>95%). The rate of this reaction is increased by the addition of imidazole to 3.7×10^{-4} M. Furthermore, on addition of ABTS to a concentration of 1.0×10^{-3} M, the manganese(IV)–oxo species is rapidly reduced to manganese(III) porphyrin. At pH >12.5, formation of a manganese(IV)–oxo species is complete[21] ($\lambda_{max} = 422$ nm, $\epsilon_{max} = 8.6$

(20) Carnieri, N.; Harriman, A.; Porter, G.; Kalyanasundaram, K. *J. Chem. Soc., Dalton Trans.* **1982**, 1231.

$\times 10^4$) upon addition of hydrogen peroxide (Figure 8B). The addition of ABTS, after formation of the manganese(IV)–oxo species, results in the reduction of the manganese(IV)–oxo species to regenerate manganese(III) porphyrin without the formation of appreciable $ABTS^{\bullet+}$. Since at this pH $ABTS^{\bullet+}$ is quantitatively formed on turnover of HOO^- with manganese(III) porphyrin, one must conclude that 20 equiv of H_2O_2 has reacted with the higher valent manganese–oxo species during the period of time between addition of hydrogen peroxide and ABTS. Thus, in the absence of ABTS as a trap at high pH, HOO^- is radidly oxidized to O_2 and H_2O, and manganese(V)–oxo porphyrin is reduced to manganese(III) porphyrin. Imidazole (4.2×10^{-4} M) accelerates this process.

Discussion

The reaction of hydrogen peroxide with a manganese(III) tetraphenylporphyrin has been investigated. For this purpose we have used the water-soluble aquo-ligated [5,10,15,20-tetrakis-(2,6-dimethyl-3-sulfonatophenyl)porphinato]manganese(III) ((**1**)Mn^{III}(X), where X = H_2O or HO^-) (H_2O solvent, 30 ± 0.1 °C, μ = 0.23; with $H_2PO_4^-/HPO_4^{2-}$, HCO_3^-/CO_3^{2-}, 2,4,6-collidine hydrochloride/2,4,6-collidine, and H_2O/HO^- as buffers). (**1**)-Mn^{III}(X) is soluble in water and is sterically blocked to μ-oxo dimer formation. The kinetics of the reaction were studied by competitively trapping the reactive higher valent manganese–oxo species with ABTS and hydrogen peroxide (Scheme I). In Scheme I catalyst refers to (**1**)$Mn^{III}(H_2O)$ or (**1**)Mn^{III}(OH) and HP refers to H_2O_2 or HO_2^- dependent upon pH, while [catalyst=O]$^+$ and [catalyst=O] refer to manganese–oxo porphyrin species at a particular pH that are 2e and 1e oxidized above the manganese(III) porphyrin state. Reactions were monitored by following the appearance of $ABTS^{\bullet+}$ with time. With or without imidazole (ImH) ligation the reaction is first order in the concentration of both manganese(III) porphyrin and hydrogen peroxide and zero order in [ABTS]. These results establish the rate-limiting step (k_{rds}, Scheme I) to involve transfer of an oxygen atom from hydrogen peroxide to the metal center of the manganese(III) porphyrin. Also, at given pH values the pseudo-first-order rate constants (k_{obsd}) for the formation of $ABTS^{\bullet+}$ and O_2 are, within experimental error, identical.

Scheme I

$$\text{catalyst} + \text{HP} \underset{}{\overset{K_q}{\rightleftharpoons}} \text{catalyst(HP)}$$

$$\text{catalyst(HP)} \xrightarrow{k_{rds}} [\text{catalyst=O}]^{1+} + \text{H}_2\text{O (or HO}^-\text{)}$$

$$[\text{catalyst=O}]^{1+} + \text{ABTS} \xrightarrow{\text{fast}} [\text{catalyst=O}] + \text{ABTS}^{\bullet+} + \text{H}^+$$

$$[\text{catalyst=O}] + \text{ABTS} \xrightarrow{\text{fast}} [\text{catalyst}] + \text{ABTS}^{\bullet+} + \text{H}_2\text{O}$$

$$[\text{catalyst=O}]^{1+} + \text{HP} \xrightarrow{\text{fast}} [\text{catalyst}] + \text{O}_2 + \text{H}_2\text{O}$$

The influence of pH on the reaction is shown in the pH vs log of the pH-dependent apparent second-order rate cosntant (k_{1y}) profiles of Figure 6, parts A and B. The line for Figure 6A has been generated from eq 12, while the line of Figure 6B was generated from eq 13. Terms A and B of eq 12 are for the reaction of HO_2^- with (**1**)$Mn^{III}(H_2O)_2$ and with (**1**)Mn^{III}(OH)(H_2O), respectively. For Figure 6B the correlation line has been generated from eq 13, which contains the three terms C–E. These terms pertain to the following reactions: C, H_2O_2 + (**1**)$Mn^{III}(H_2O)$(-HO); D, HO_2^- + (**1**)$Mn^{III}(H_2O)$(HO); E, HO_2^- + (**1**)Mn^{III}(OH)$_2$.

Visual inspection of Figure 6, parts A and B, shows that 6B would appear best, and this is supported by the standard deviation of the fit for 6A being 0.183 as compared with that for 6B of 0.117. In the fit for Figure 6A it is assumed that there is only one proton dissociation of a water ligand (pK_a = 12.43). No other acid dissociation is seen by spectral titration of (**1**)$Mn^{III}(H_2O)_2$ in the range pH 3–11. The fit of eq 13 to Figure 6B involves the assumption (eq 15) of two proton dissociations (pK_a = 8.2 and 12.50). These may be compared with the titrimetric pK_a values

$$(\mathbf{1})\text{Mn}^{\text{III}}(\text{OH}_2)(\text{OH}_2) \underset{}{\overset{pK_{a1}}{\rightleftharpoons}} (\mathbf{1})\text{Mn}^{\text{III}}(\text{OH}_2)(\text{OH}) + \text{H}^+ \quad (15)$$

$$(\mathbf{1})\text{Mn}^{\text{III}}(\text{OH}_2)(\text{OH}) \underset{}{\overset{pK_{a2}}{\rightleftharpoons}} (\mathbf{1})\text{Mn}^{\text{III}}(\text{OH})(\text{OH}) + \text{H}^+$$

of 8.6 and 11.6 reported by Harriman[12] for the aquo species of [5,10,15,20-tetrakis(4-sulfonatophenyl)porphinato]manganese(III) hydrate. Apparently the molar extinction coefficients of (**1**)-$Mn^{III}(H_2O)_2$ and (**1**)$Mn^{III}(H_2O)$(HO) do not differ sufficiently to determine the lower pK_a by spectrophotometric titration. The calculated rate constants (M^{-1} s^{-1}) accompany structures that describe the composition of the critical transition states for oxygen transfer to manganese(III) porphyrin (Chart III). The kinetically equivalent ($v = k'[(\mathbf{1})\text{Mn}^{\text{III}}(\text{HO})][H_2O_2]$ and $v = (k'K_a/K_0)$-$[(\mathbf{1})\text{Mn}^{\text{III}}(H_2O)(HO_2^-)]$, where K_a and K_0 represent the acid dissociation constants of (**1**)$Mn^{III}(H_2O)_2$ and H_2O_2, respectively) structure Ib is likely the most stable based upon the basicity of the ligated oxygen of hydroxyl and hydroperoxide moieties.[10]

Imidazole Ligation to Manganese(III) Porphyrin Increases Its Rate of Oxidation by Hydrogen Peroxide. The manganese(III) porphyrin ligates only one imidazole (ImH). There is precedence in the literature[22] for only monoligation of manganese(III) porphyrin by ImH. The equilibrium constant for ImH ligation was determined (log K_1 = 2.20 ± 0.05) by spectral titration between pH 6.0 and 7.5 at μ = 1.0 and by kinetic means (log K_1 = 2.90 ± 0.05) between pH 7.6 and 10.2 at μ = 0.23. The difference in the determined values of K_1 may arise from the difference in ionic strength for the two means of determination.[23] A knowledge of the value of K_1 is not required in the kinetic analysis. Throughout the entire pH range, the reaction of the ImH ligated manganese(III) porphyrin is with hydrogen peroxide anion (eq 16). The second-order rate constants Kk (calculated from the

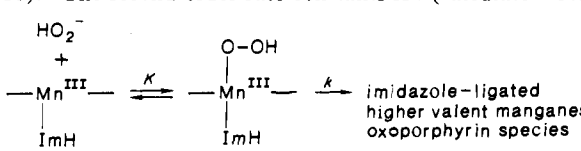

(16)

inset) to the plot of Figure 6B) of 5.6×10^5 M^{-1} s^{-1} may be compared with the rate constant when HO^- rather than ImH serves as the axial ligand ($k_3 = 5.3 \times 10^4$ M^{-1} s^{-1}). It follows that with ImH ligation the rate is ~10-fold greater. This is so from pH 7.6 to 10.2 by comparison of Figure 6A and the inset to Figure 6B. The displacement of both H_2O and HO^- axial ligands by imidazole is not surprising, because nitrogen bases have stronger trans effects in substitution reactions than do HO^- and H_2O ligands.[24]

In previous studies from this laboratory it has been shown that oxygen transfer from percarboxylic acids and alkyl hydroperoxides (YOOH) to (TPP)$Mn^{III}Cl$[25a] is much faster with ImH ligation. The rate enhancement due to imidazole ligation was found to be of the order of 10^3–10^4 in methylene chloride solvent. A large rate enhancement accompanying ImH ligtaion has also been seen in the reaction of (Me_8TPP)$Mn^{III}Cl$[25b] with *p*-cyano-*N*,*N*-dimethylaniline *N*-oxide (NO). The very small rate enhancement (only 10-fold) observed in the present system may be understood by inspection of eq 17a–c. The displacement of H_2O from

(21) (a) Carnieri, N.; Harriman, A.; Porter, G. *J. Chem. Soc. Dalton Trans.* **1982**, 931. (b) Hill, C. L.; Schardt, B. C. *J. Am. Chem. Soc.* **1980**, *102*, 6374. (c) Camenzind, M. J.; Hollander, F. J.; Hill, C. L. *Inorg. Chem.* **1982**, *21*, 4301. (d) Smegal, J. A.; Schardt, B. C.; Hill, C. L. *J. Am. Chem. Soc.* **1983**, *105*, 3510. (e) Camenzind, M. J.; Hollander, F. J.; Hill, C. L. *Inorg. Chem.* **1983**, *22*, 3776. (f) Groves, J. T.; Kruper, W. J., Jr.; Haushalter, R. C. *J. Am. Chem. Soc.* **1980**, *102*, 6375. (g) Groves, J. T.; Watanabe, Y.; McMurry, T. J. *J. Am. Chem. Soc.* **1983**, *105*, 4489. (h) Bartolini, O.; Meunier, B. *J. Chem. Soc., Chem. Commun.* **1983**, *1364*. (i) Mansuy, D.; Battioni, P.; Renaud, J.-P. *J. Chem. Soc., Chem. Commun.* **1984**, 1255.

(22) Neya, S.; Morishima, I.; Yonezawa, T. *Biochemistry* **1981**, *20*, 2610.
(23) Lenz, G. R.; Martell, A. E. *Inorg. Chem.* **1965**, *4*, 379.
(24) Cotton, F. A.; Wilkinson, G. In *Advanced Inorganic Chemistry*, 4th ed.; Wiley: New York, 1980, p 1200.
(25) (a) Yuan, L.-C.; Bruice, T. C. *J. Am. Chem. Soc.* **1986**, *108*, 1643. (b) Wong, W. H.; Ostovic, D.; Bruice, T. C. *J. Am. Chem. Soc.* **1987**, *109*, 3428.

$$(TPP)Mn^{III}(ImH)(Cl) + YOOH \rightleftarrows (TPP)Mn^{III}(ImH)(YOOH) + Cl^- \quad (17a)$$

$$(Me_8TPP)Mn^{III}(ImH)(Cl) + NO \rightleftarrows (Me_8TPP)Mn^{III}(ImH)(NO) + Cl^- \quad (17b)$$

$$(1)Mn^{III}(ImH)(H_2O) + HOO^- \rightleftarrows (1)Mn^{III}(ImH)(HO_2) + H_2O \quad (17c)$$

$(1)Mn^{III}(OH_2)(ImH)$ by HOO^- is more difficult than is the displacement of Cl^- by NO or YOOH species (eq 17a,b) in organic aprotic solvents. Manganese(III) porphyrins are known to bind preferentially to oxygen donor rather than nitrogen donor ligands. In aqueous solutions the ligands N_3^-, NCS^-, and CN^- do not complex with manganese(III) hematoporphyrin IX, (HPorph)-$Mn^{III}(OH)(OH_2)$.[26]

Absence of General-Base Catalysis. Below saturation in ImH, k_{obsd} increases linearly with increase in [ImH], and at saturating concentrations of ImH, k_{obsd} is independent of [ImH]. Therefore, ImH does not act as a general-base catalyst in the oxidation of ImH-ligated manganese(III) porphyrin by oxygen transfer from HOO^-. The oxyanions HPO_4^{2-}, HCO_3^-, and CO_3^{2-} are also not catalysts. It should be noted here that 2,4,6-collidine catalyzes the reaction of $(1)Fe^{III}(X)$ (X = H_2O or HO^-) with hydrogen peroxide (see the introduction).[10] The influence of 2,4,6-collidine on the rate of reaction of $(1)Mn^{III}(X)$ with hydrogen peroxide was studied between pH 7.59 and 9.0, where the predominant species is I. With Ia (Chart III), transfer of the H–OOH proton (eq 18) should, in analogy with $(1)Fe^{III}(X)$, be expected to increase the rate of oxygen transfer and H_2O departure. However, at pH

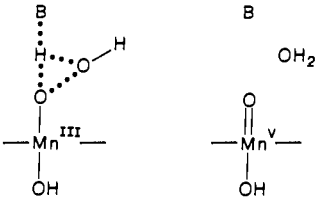

(18)

8.34 there is no significant change in k_{obsd} for a 33-fold change in the concentration of 2,4,6-collidine/2,4,6- collidine hydrochloride buffer. Lack of general-base catalysis by imidazole and 2,4,6-collidine may be explained, if one assumes that the structure Ib rather than Ia predominates. Another plausible explanation would be that the species $(1)Mn^{III}(OH)(HOOH)$ undergoes initial homolytic cleavage by the mechanism of eq 19. For such a mechanism there is no need for general-base catalysis.

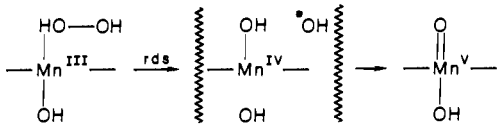

(19)

It may be recalled[10] that catalysis was not observed for oxyanion bases such as carbonate, phosphate, acetate, and chloroacetate with $(1)Fe^{III}(X)$. This was explained by a favorable electrostatic interaction (Chart II) in the transition state for the neutral amine catalyst and electrostatic repulsion with oxyanion bases. It was pointed out, however, that the observation of an increase in rate with a single agent (2,4,6-collidine) does not truly establish the phenomenon as general-base catalysis.

Comparisons of the Rates of Reaction of $(1)Mn^{III}(X)$ and $(1)Fe^{III}(X)$ with Hydrogen Peroxide in the Absence of ImH. Since the reaction of the manganese(III) porphyrin with hydrogen peroxide could not be studied at pH <7.5 due to the slowness of the reaction and low yield of $ABTS^{\bullet+}$, one is not able to compare the rate terms $k_1[(1)Mn^{III}(H_2O)_2][H_2O_2]$ with that of $k_1'[(1)Fe^{III}(H_2O)_2][H_2O_2]$ ($k_1' = 44\ M^{-1}\ s^{-1}$). Comparisons of the terms $k_2'[(1)Fe^{III}(H_2O)(HO)][H_2O_2]$ and $k_2[(1)Mn^{III}(H_2O)(HO)][H_2O_2]$ show k_2' ($1.67 \times 10^3\ M^{-1}\ s^{-1}$) to be greater than k_2 ($8.76 \times 10^1\ M^{-1}\ s^{-1}$) by approximately 19-fold. This kinetic advantage enjoyed by the iron(III) porphyrin could be due either to a more favorable ligation of hydroperoxide or a more rapid breakdown of the complex of hydrogen peroxide and iron(III) porphyrin. A comparison of the first CV oxidation potential (pH 3.25) of $(1)Fe^{III}(H_2O)_2$[10] (+0.86 V) and $(1)Mn^{III}(H_2O)_2$[27] (+1.04 V) shows that the latter is probably the most reasonable explanation. A comparison of the kinetic terms $k_3'[(1)Fe^{III}(OH)][HO_2^-]$ and $k_3[(1)Mn^{III}(OH)][HO_2^-]$ establishes that the rate constant for k_3' ($1.05 \times 10^5\ M^{-1}\ s^{-1}$) is greater than that for k_3 ($5.38 \times 10^4\ M^{-1}\ s^{-1}$) by but ~2-fold. In the reactions of the iron(III) porphyrin there is no counterpart to the term $k_4[(1)Mn^{III}(OH)_2][HO_2^-]$. The rate constant k_4 ($6.94 \times 10^5\ M^{-1}\ s^{-1}$) exceeds k_3 by but ~12-fold, though in both processes the same critical complex is formed (eq 20). This result points out the

$$(1)Mn^{III}(H_2O)(HO) + HOO^- \rightleftarrows (1)Mn^{III}(HO)(HO_2^-) + H_2O \quad (20)$$

$$(1)Mn^{III}(HO)_2 + HOO^- \rightleftarrows (1)Mn^{III}(HO)(HO_2^-) + HO^-$$

trans lability of the bis(hydroxy) ligated species with its extra negative charge. The value of k_4 is favorably comparable with the second-order rate constant ($1.9 \times 10^5\ M^{-1}\ s^{-1}$ at pH 14) reported by Harriman[21a] for the reaction of HOO^- with [*meso*-tetrakis(4-sulfonatophenyl)porphinato]manganese(III).

The pH Dependence of the Formation of the Products O_2 and $ABTS^{\bullet+}$. Scheme I pertains to the means of formation of O_2 and $ABTS^{\bullet+}$ as products. The yields of O_2 and $ABTS^{\bullet+}$ account for the hydrogen peroxide consumed. Change in pH from 7.59 to 12.0 results in an increase in the yield of $ABTS^{\bullet+}$ from 3.9% to ~100%. At the same time, the yield of O_2 decreases with increase in pH. Therefore, the higher valent manganese–oxo porphyrin species formed from Ia as compared with that from II and III preferentially oxidizes HOO^-, and the species formed from II and III preferentially carries out a 1e oxidation of ABTS. The yield of $ABTS^{\bullet+}$ also increases gradually with pH (40%, pH 7.60; 46%, pH 8.90; 55%, pH 9.30; 61%, pH 9.85; 63%, pH 10.2) on saturation with ImH, while the yield of O_2 decreases. Since the structure of the immediate product of reaction of $(1)Mn^{III}(ImH)$ with HO_2^- should be pH independent, one must assume that this higher valent manganese–oxo porphyrin is altered in some fashion dependent upon hydroxide concentration. This alteration can not involve exchange of ImH ligand for an aquo or HO^- species. Such a process would generate the higher valent manganese–oxo porphyrin species obtained from Ib and II, which would necessitate a decrease in the yield of $ABTS^{\bullet+}$ with an increase in pH. Two plausible explanations come to mind (eq 21 and 22). The hep-

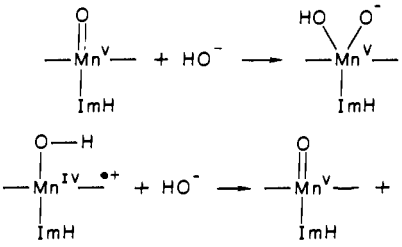

tacoordinated species of eq 21 would likely be a better outer-sphere 1e oxidant of ABTS than an oxidant of hydrogen peroxide, since the latter reaction most likely requires ligation of hydrogen peroxide; while the $Mn^V{=}O$ species of eq 22 would be the better oxidant of hydrogen peroxide.

The Specificity for 1e Oxidation of ABTS and 2e Oxidation of HOO^- As a Function of pH and ImH Ligation. At the lowest pH investigated (pH 7.6) the ratio of rate constant for oxidation of $HOO^- \rightarrow O_2 + H_2O$ exceeds that for oxidation of ABTS $\rightarrow$ $ABTS^{\bullet+}$ by a factor of 24 (as shown by the product yields). Therefore, it may be concluded that the manganese(IV)–oxo π-cation radical is best at the oxidation of H_2O_2, while the manganese(V)–oxo porphyrin species (formed at pH >11.5) ox-

(26) Boucher, L. J. *Coord. Chem. Rev.* **1972**, *7*, 294.

(27) (a) Lee, R. W.; Bruice, T. C., unpublished results. (b) Calderwood, T. S.; Bruice, T. C., unpublished results.

Chart III

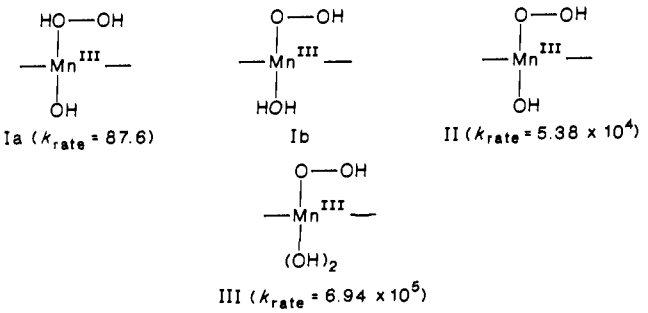

idizes ABTS in preference to H_2O_2. The manganese(III) of structure Ia should be of high spin, and HOO^- need only compete with water for ligation. At the intermediate pH of 10.2, HOO^- is oxidized only two times faster than is ABTS. At this pH, HOO^- need only compete with water for ligation; however, comparison of structures Ia and II suggests that the manganese moiety of the latter should be of lower spin. A decrease in spin state is proposed to result in the preferential oxidation of ABTS over HOO^-. At pH 12.0 there is formed no more than 10% O_2. The change in relative rates of formation of O_2 and $ABTS^{\bullet+}$ in going from pH 10.2 to 12.0 amounts to a $\Delta\Delta G^{\ddagger}$ of but 0.65 kcal·M^{-1}. Such small differences in free energies of activation are most difficult to explain in terms of mechanism. The increase in rate of $ABTS^{\bullet+}$ formation over O_2 on going from pH 10.2 to 12.0 with ImH as an axial ligand or at pH 10.2 by adding ImH as an axial ligand amounts, in both cases, to an even smaller change in $\Delta\Delta G^{\ddagger}$ (0.4 kcal·M^{-1}).

It should be noted that there is a distinct difference in the dependence of yield of O_2 and $ABTS^{\bullet+}$ upon pH for (**1**)$Mn^{III}X$ compared with the (**1**)$Fe^{III}X$.[10] With the former, preference for ABTS oxidation is seen at high pH, whereas with the latter ABTS oxidation is favored over H_2O_2 oxidation at low pH. This shows that at higher pH higher valent manganese–oxo species prefer to undergo two one-electron reductions (thereby producing two $ABTS^{\bullet+}$ radical species), whereas the iron(IV)–oxo π-cation radical more easily undergoes a single two-electron reduction. In the presence of water the potentials for the iron(III)–oxo porphyrin/iron(IV)–oxo porphyrin and iron(IV)–oxo porphyrin/iron(IV)–oxo porphyrin π-cation radical are superimposable.[28]

Identification of Higher Valent Manganese–Oxo Porphyrin Species by Repetitive Spectral Scanning (350–700 nm) during the Course of the Reaction. In the absence of ABTS and ImH at pH 7.59 a buildup of a higher valent manganese–oxo porphyrin species is not observed, and the catalyst remains at the manganese(III) oxidation state throughout the reaction. Under the same conditions at pH 12.5 the manganese(III) porphyrin is quantitatively converted to a manganese(IV)–oxo species (λ_{max} 422 nm, ϵ 8.6 × 10^4 M^{-1} cm^{-1}). This observation supports the previous finding that high-valent Mn–oxo species (both Mn(IV) and Mn(V)) are stabilized by hydroxide ion ligation.[20,29] Thus, it has been shown by electrochemical methods that the exchange of H_2O for HO^- as axial ligand is accompanied by the conversion of manganese(III) porphyrin π-cation radical to manganese(IV) porphyrin.[30] The formation of manganese(IV)–oxo porphyrin above ~pH 11.5 may be explained by the trapping of manganese(V) by unreacted manganese(III) porphyrin (eq 23). The comproportionation reaction of eq 23 is eminently reasonable. Thus, manganese(V) porphyrin carries out a 1e oxidation of ABTS.

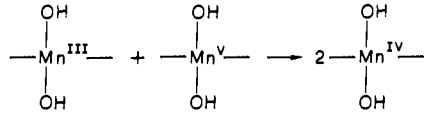

(23)

Acknowledgment. This work was supported by the National Institutes of Health and National Science Foundation.

(28) (a) Lee, W. A.; Calderwood, T. S.; Bruice, T. C. *Proc. Natl. Acad. Sci. U.S.A.* **1985**, *82*, 4301. (b) Calderwood, T. S.; Lee, W. A.; Bruice, T. C. *J. Am. Chem. Soc.* **1985**, *107*, 8272. (c) Calderwood, T. S.; Bruice, T. C. *Inorg. Chem.* **1986**, *25*, 3722.
(29) Calvin, M. *Rev. Pure Appl. Chem.* **1965**, *15*, 1.
(30) Spreer, L. O.; Maliyackel, A. C.; Holbrook, S.; Otvos, J. W. Calvin, M. *J. Am. Chem. Soc.* **1986**, *108*, 1949.

Communications to the Editor

The First α-Silicon-Substituted Simple Enol. The Stabilizing Effect of the Silyl Substituent

Ella B. Nadler and Zvi Rappoport*

Department of Organic Chemistry, The Hebrew University Jerusalem 91904, Israel

Dorit Arad and Yitzhak Apeloig*

Department of Chemistry, Technion-Israel Institute of Technology, Haifa 32100, Israel

Received June 18, 1987

There is considerable current interest in both organosilicon chemistry[1] and in simple enols.[2] A combination of our interests[3,4] in these fields led to isolation of the first stable simple α-silyl enol, which shows a remarkable stability relative to the corresponding keto isomer in comparison with the corresponding α-alkyl analogues.

In Jerusalem we had recently studied a group of highly congested enols of the general type **1** (Mes = mesityl) which exhibit an unusually high kinetic and thermodynamic stability.[3] The keto ⇌ enol equilibrium constants (K_{Enol} = [**1**]/[**2**]) in hexane depend on the α-substituent. For aliphatic R's K_{Enol} decreases with the increased bulk of R from 20 for R = H to 0.64 for R = Me (**1a**) to 0.06 for R = *t*-Bu (**1b**).[3b] For R = meta- and para-substituted α-aryl groups K_{Enol} decreases with electron donation (0.3 for *p*-anisyl) and increases with electron withdrawal (3.6 for R = 3,5-$Br_2C_6H_3$).[3c] For bulky α-aryl groups K_{Enol} is higher (79 for R = Mes).[3a]

Can a "simple" substituent (e.g., not strongly electron withdrawing) be found which will increase K_{Enol} above the values for R = alkyl and ortho-substituted aryl groups? Our studies in Haifa of organosilicon compounds provided an answer. Silicon is less electronegative than carbon,[5] and as expected from the above data,

(1) (a) Chvalosky, V.; Bellama, J. M. *Carbon-Functional Organosilicon Compounds*; Plenum Press: New York, 1984. (b) Fleming, I. In *Comprehensive Organic Chemistry*; Barton, D., Ollis, W. D., Eds.; Pergamon Press: Oxford, 1979; Vol. 3, p 541.
(2) (a) Toullec, J. *Adv. Phys. Org. Chem.* **1982**, *18*, 1. (b) For a recent reference, see: Chiang, Y.; Hojatti, M.; Keefe, J. R.; Kresge, A. J.; Schepp, N. P.; Wirz, J. *J. Am. Chem. Soc.* **1987**, *109*, 4000.
(3) (a) Biali, S. E.; Rappoport Z. *J. Am. Chem. Soc.* **1985**, *107*, 1007. (b) Nugiel, D. A.; Rappoport, Z. *Ibid.* **1985**, *107*, 3369. (c) Nadler, E. B.; Rappoport, Z. *Ibid.* **1987**, *109*, 2112.
(4) (a) Apeloig, Y.; Stanger, A. *J. Am. Chem. Soc.* **1985**, *107*, 2806. (b) Apeloig, Y.; Stanger, A. *J. Org. Chem.* **1982**, *47*, 1462; **1983**, *48*, 5413. (c) Stanger, A. Ph.D. Thesis, Technion, Haifa, Israel, 1985.

0002-7863/87/1509-7873$01.50/0